

VSAERO Implementation within the ANSA Environment

¹Yash Khandhia, ²Anna Robinson

¹Applied Computing & Engineering Ltd., England, ²Stark Aerospace, Inc. Analytical Methods Division, USA

KEYWORDS –

Preliminary aerodynamic design, Computational Fluid Dynamics

ABSTRACT –

This paper proposes the incorporation of the VSAERO software into the ANSA environment. VSAERO has been a widely accepted surface singularity panel method used for preliminary design in the aircraft, naval and automotive industries for the past 30 years. The method rapidly computes the nonlinear aerodynamic characteristics of arbitrary configurations in subsonic flow. The addition of this functionality to ANSA has the potential to increase the scope of ANSA's capabilities in the field of preliminary aerodynamic design.

The user will be able to run VSAERO simply by means of a mouse prompt within ANSA. They will then have the option to modify the basic data that controls the functionality of VSAERO. ANSA will internally generate the input file, execute VSAERO and display the final result in the ANSA post processor.

The integration will also involve adding wake creation capability in ANSA. Wake data is necessary for VSAERO to calculate the aerodynamic properties of lifting surfaces. These modeling features consist of thin sheets defined by quadrilateral elements that originate from component edges.

The integration of these two complementary programs will create a more efficient user experience by combining the functionality of several different programs into one environment.

TECHNICAL PAPER –

1. INTRODUCTION

Due to the increasing competition and demands to reduce costs and improve efficiency, companies benefit from tools that streamline the preliminary design and analysis process. By incorporating VSAERO, a proven preliminary design tool, into the ANSA environment we can provide the user with an efficient and easily automatable software package.

VSAERO has been established in the aerospace, naval and automotive industries for more than three decades. The software system and VSAERO technology, which quickly calculates the nonlinear aerodynamic characteristics of arbitrary configurations in subsonic flow, are considered design standards from concept through preliminary and final design in many major companies.

The integration of VSAERO will also allow ANSA to expand its market into the traditional VSAERO customer base as well as industries to which VSAERO is quite suited yet underused, such as renewable energy. Currently, there is a global drive to develop alternative energy sources due to increasing conventional energy costs. Considerable research funding is expended for increasing the efficiency of wind turbines and developing new designs for tidal

energy generation devices. In order to assess a large number of design cases, which is necessary to arrive at innovative solutions, there is a strong need for Computational Fluid Dynamics (CFD) methods which can rapidly provide accurate analysis. VSAERO is a perfect tool for these applications.

The VSAERO simulation method requires structured quadrilateral or unstructured triangular surface grids which can be rapidly generated in ANSA and the analysis results can be evaluated using the built in post processing capability. The scripting (journaling) capability of ANSA will allow batch execution of VSAERO which will be necessary for running optimization studies.

The addition of VSAERO into the ANSA environment will allow the user easy access to VSAERO tools, all while only running one program, ANSA. Much of the process of using VSAERO currently, including importing and exporting different file types, will happen behind the scenes, creating a streamline feel for the user. Within ANSA, VSAERO will be available via a deck option and all user input options will be accessible through changeable menus.

2. VSAERO IN THE ANSA ENVIRONMENT

The current process to use VSAERO as a standalone program requires that the user generate a VSAERO input file, usually through gridding software. This input file consists of basic data, body geometry and wake geometry and can be modified directly through a text editor or through SPIN(w), a wake generation software. The user can then run VSAERO and view the output with a text editor or graphical post-processor.

While working in ANSA, the user will be able to select the VSAERO deck option, which will include a menu for use in preparing the model to run in VSAERO. This will allow the user to easily modify the basic data, which includes general information, onset flow and reference conditions, through a simple menu. With a button click, a display window will show the current basic data setting and allow the user to make changes.

The creation of wake data is also necessary in order to run VSAERO. Wakes consist of thin sheets defined by quadrilateral elements that originate from component edges. The user will be able to add wakes by clicking a wake generation button and selecting the model component to which the wake will be attached. The stream wise wake lines will originate from the grid nodes and a wake menu will allow the user to specify the density and distribution of the perpendicular wake lines that form the quadrilateral elements.

Once the model has been prepared, the user will be able to run VSAERO with the push of a button and import the results into ANSA's post-processor.

3. VSAERO CAPABILITIES

VSAERO¹ is a subsonic panel method that has evolved over the past 30 years. The public domain version² was limited to external flow problems of 1000 panels or less. Version 7 has solved problems with 70 thousand panels. The code has been rewritten in the past 20 years based upon customer experience. The first priority has been to produce a robust code, followed by accuracy, versatility, speed and simplicity. Notable additions include: internal flows³, body wakes, added mass, non-uniform inflow, free surfaces⁴, warped panels⁵, boundary layer coupling, unstructured grids of triangular panels⁶, induced drag analysis⁷, and oscillatory flows⁸.

VSAERO applications include (Figure 1): aircraft, cars, sailboats, ships, and wind turbines. Typical model sizes are 10-20 thousand panels with compute times of minutes on a desktop PC.

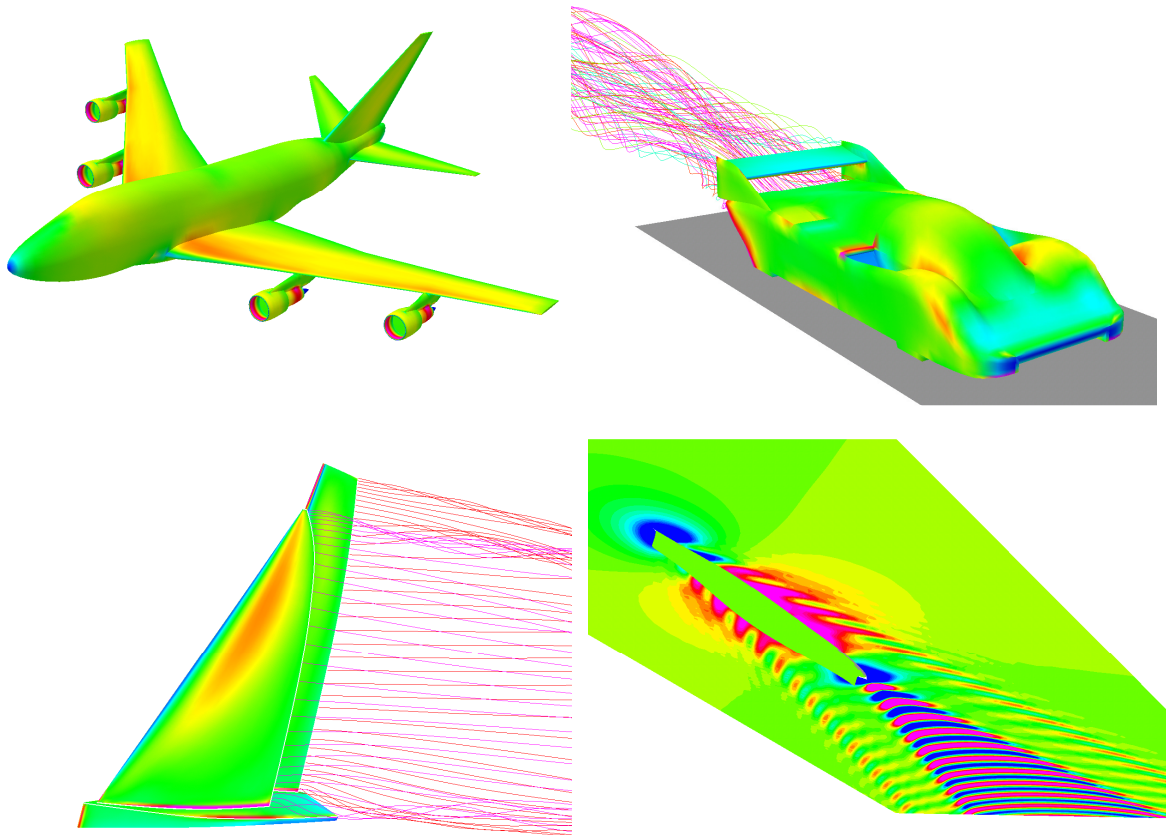


Figure 1 – VSAERO applications

VSAERO solves for the perturbation potential ϕ on the body surface through the boundary integral equation

$$2\pi\phi(p) + \int_{S-p} \phi \frac{\partial}{\partial n} \left(\frac{1}{r} \right) dS = \int_S \frac{\partial \phi}{\partial n} \frac{1}{r} dS \quad (1)$$

Point p is on the body surface S and r is the distance from p to the arc dS where the normal n points into the flow. Eq. (1) applies to arbitrary shapes, and VSAERO is unrestricted as to the body geometry. The accuracy with which Eq. (1) is solved and whether the actual flow meets the restrictions in the derivation of Eq. (1) determine how well VSAERO matches experiment. The assumptions inherent in Eq. (1) are the same as those required to derive Laplace's equation; that is, disturbance velocities are small compared to the speed of sound and vorticity is confined to the thin boundary layer on the body or zero-thickness *wake* surfaces. Eq. (1) is simply Green's Identity and was first coded by Morino⁹.

Compared to Navier-Stokes codes, the absence of viscosity in potential flow would appear to be physically unrealistic. For example, the vortices trailing behind an aircraft persist indefinitely

according to potential flow. However, numerical viscosity in the more complex codes often dissipates vorticity much too rapidly causing significant error in the flow influenced by the wake, as is the case for the downwash on the tail of an airplane or the blade/vortex interaction of a helicopter. Fundamentally, the advantages of a panel method are a single scalar equation describing the flow and a mesh that is only two dimensional, not three dimensional, and therefore easier to generate.

The normal derivative of the potential on the body surface is a user-specified velocity plus the normal components of the rotational velocity and freestream, and the transpiration due to boundary-layer thickness.

$$\frac{\partial \phi}{\partial n} = -V_{\text{norm}} + (\mathbf{V}_{\text{onset}} - \boldsymbol{\omega} \times \mathbf{r}) \cdot \mathbf{n} + \frac{\partial}{\partial s}(V\delta^*) \quad (2)$$

The user-specified velocity is zero for solid surfaces, but non-zero for radiators, engine inlets and exhausts. Obviously, VSAERO solves the Neumann problem of potential flow. The advantage of recognizing VSAERO as a Neumann solver is that the modifications necessary to solve an internal flow are well known and were easily implemented by Nathman³. Internal flows occur not just inside ducts but also result from closed separation bubbles such as the wake behind a bluff body and the exhausts of jet engines. The technique for handling internal flows has led to improved models of bluff body wakes.

Wakes are part of the boundary because they contain vorticity. The difference in potential across the wake sheet is determined (for wakes separating fluids with the same total energy) by the potential on the body from where the wake emanates,

$$\Delta \phi = \phi_u - \phi_l + V_\infty \cdot (\mathbf{r}_u - \mathbf{r}_l) \quad (3)$$

Eq. (1) is converted to a matrix equation,

$$[A] \{ \phi \} = [B] \left\{ \frac{\partial \phi}{\partial n} \right\} \quad (4)$$

by dividing the boundary into elements (panels) in which the potential and its normal derivative are defined by polynomials with unknown coefficients. Each panel has a potential distribution

$$\phi = \phi_0 + \phi_x x + \phi_y y \dots \quad (5)$$

where x and y are local distances from the panel control point. In the original scheme, the polynomial is truncated to the first term; thus the first version of VSAERO was a low-order method. PANAIR¹⁰ is a higher-order method because it uses second order polynomials. VSAERO Version 7 is multi-order in that parts of the surface are represented by low-order distributions while other parts include the linear terms in Eq. (5). The velocities on the body surface are determined in VSAERO by differentiating the potential.

Structured patches are $m \times n$ networks of quadrilateral panels. It is easier to work with 100 patches than 10,000 individual panels; fewer patches reduce a user's workload. By definition, a structured patch cannot have a hole inside, or mismatched panels. Figure 2 is a Formula 1 rear wing endplate with three overlapping airfoil elements. It illustrates the structured grids

exclusively used in VSAERO prior to Version 7. A dozen structured patches as indicated by different colors are required to accommodate the three holes and variation in panel size from the trailing edge of the smallest airfoil to the edge of the endplate.

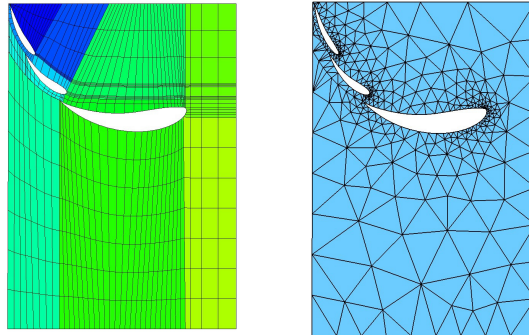


Figure 2 – Structured and Unstructured Endplates

A single unstructured patch suffices for the endplate. Unstructured patches are sets of unordered triangle panels. Unstructured grids can have holes in the grid interior. Unstructured grids are increasingly advantageous as the number of intersecting elements proliferates, that is, as the body topology becomes complex. The primary advantage is that it is no longer necessary to decide how to break the endplate into rectangular, structured meshes. The second advantage is that panel size can be varied smoothly from the dense airfoils to the sparse edges of the endplate. Finally, it is trivial to match panels along patch edges to avoid gaps at the patch edge.

Including warp is useful because the aerodynamic solution is much more tolerant of rapid changes in panel size. Eliminating small panels next to big panels reduces the error from the flat-panel approximation because the control points are less likely to be inside the small radius of action of the warp. However, for structured quadrilateral panels it is impractical to expect all the panels to be the same size in often-occurring situations like wingtips, fairings and nacelle corners⁴.

Figure 3 shows a wing with an endplate having a structured grid. Figure 4 shows the wing with an unstructured endplate. A structured grid is used at the endplate trailing edge where the wake is attached. This wing was tested in a wind tunnel with several endplate configurations¹¹. Endplate 'N' is the model analyzed here. The topography of this endplate on a single wing element is much simpler than that of the Formula 1 rear race wing with three overlapping airfoil elements,

The induced drag of the wing, with and without endplate is shown in Figure 5. The behavior compares well with experiment and is the same whether the endplate is structured or unstructured.

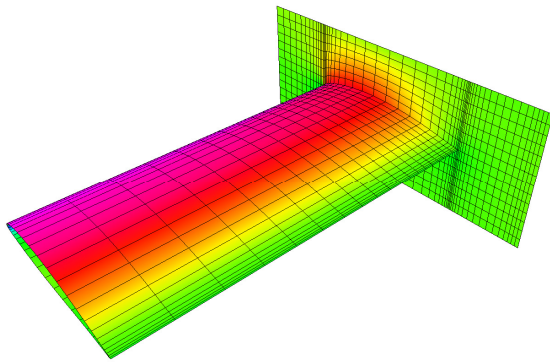


Figure 3 – Wing with Structured Endplate

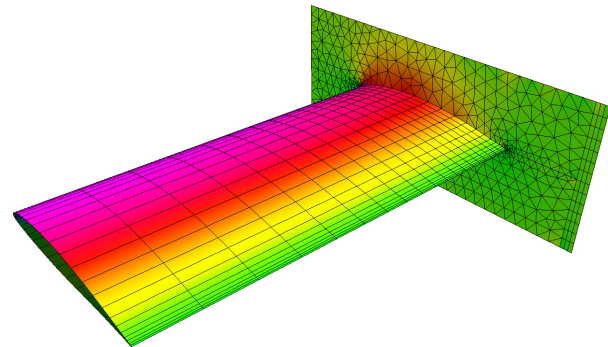


Figure 4 – Wing with Unstructured Endplate

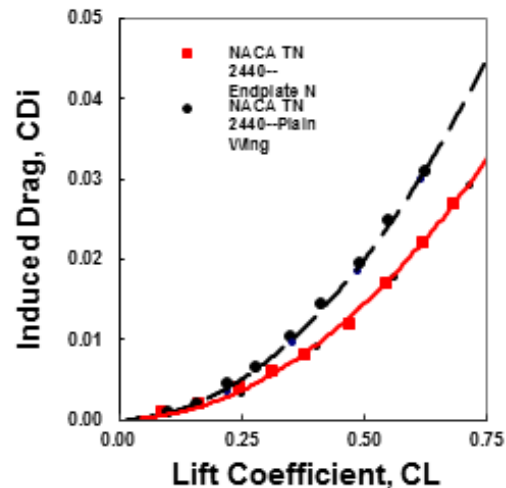


Figure 5 – Comparison of Induced Drag for Wing with and without Endplate N

Figure 6 shows the ONERA M5 model with 31 structured grids. Figure 7 shows the same model with 10 hybrid grids. Unstructured grids are used where the wing and tail intersect the fuselage. The topology of the hybrid grid is simpler because the aft fuselage can be modeled by a single unstructured patch even though the vertical and horizontal tails intersect it. The structured model has 15 grids for the aft fuselage. The unstructured grid has exactly matched panels where the aft fuselage touches the forward fuselage, fuselage base, vertical tail and horizontal tail. Some mismatch in paneling is present in the structured model. No significant difference in forces between the two.

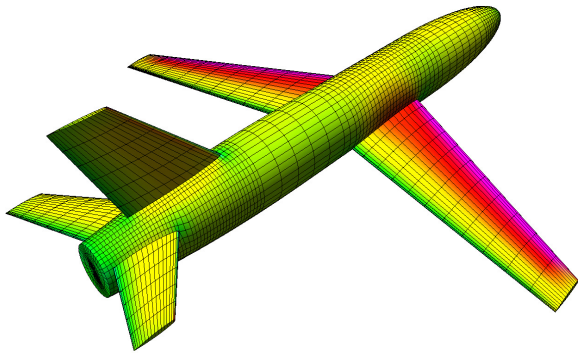


Figure 6 – ONERA M5 with Structured Grid

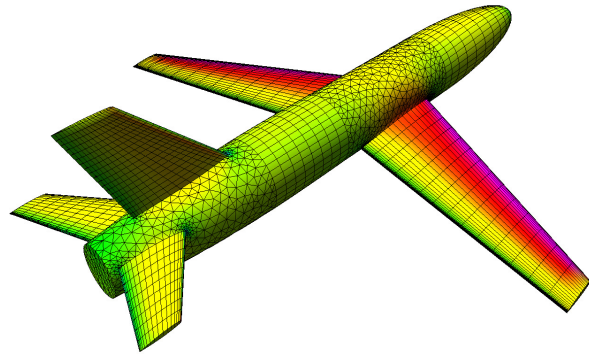


Figure 7 – ONERA M5 with Hybrid Grid

VSAERO Results

The subject geometry is the Common Research Model (CRM)¹², developed jointly by NASA's Subsonic Fixed Wing (SFW) Aerodynamics Technical Working Group (TWG) and the AIAA Drag Predictions Workshop Organizing Committee. The CRM is representative of a modern transonic commercial transport airplane, and was designed in the full configuration with a low wing, body, horizontal tail, and engine nacelles mounted below the wing. Pertinent geometric parameters are listed in Table 1. For this paper, only the wing-body configuration was used. A rendering of the geometry is shown in Figure 8, along with a photo of the wind tunnel model installed in the NASA Ames 11ft Transonic Wind Tunnel (with horizontal tail). The CRM was the subject geometry for the 4th and 5th AIAA Drag Prediction Workshops^{13, 14}.

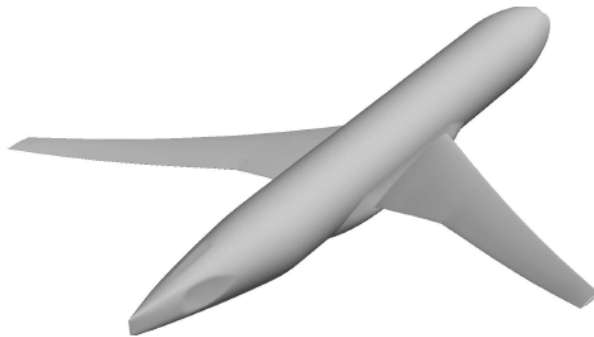


Figure 8 – NASA Common Research Model Geometry

Table 1 – Reference Quantities for the CRM

S_{ref}	594,720.0 in ² = 4,130 ft ² [458.89 m ²]	X_{ref}	1,325.9 in [33.68 m]
S_{trap}	576,000.0 in ² = 4,000 ft ² [444.44 m ²]	Y_{ref}	468.75 in [11.91 m]
b	2,313.5 in = 192.8 ft [58.765 m]	Z_{ref}	177.95 in [4.520 m]
c_{ref}	275.800 in = 16.07 ft [4.8978 m]	$\Lambda_{C/A}$	35.0°
AR	9.0	λ	0.275

An experimental investigation of the NASA Common Research Model was conducted both in the NASA Langley National Transonic Facility and NASA Ames 11-foot Transonic Wind Tunnel Facility. Data taken at these facilities included model forces and moments, wing pressures and wind tunnel model wing twist and deflections under various flow conditions. In spite of being built of high strength steel the wing of a wind-tunnel model will deflect and twist under aerodynamic load. The measured twist along the span of the wing is shown for several different angles of attack in Figure 9. In a study that demonstrated using a measured wing twist rather than the as-built model twist¹⁵, CFD analysis was based on just one twist distribution that corresponded to that at the “cruise” flight condition. This study will look at varying the twist distribution at each angle-of-attack analyzed. Ideally the solutions would be the result of coupled aerodynamic/structural aeroelastic calculations. In this case, however, measured twist increments will be used at each angle of attack analyzed. Either way a reliable process to modify the surface geometry inputs to the CFD analysis code is needed.

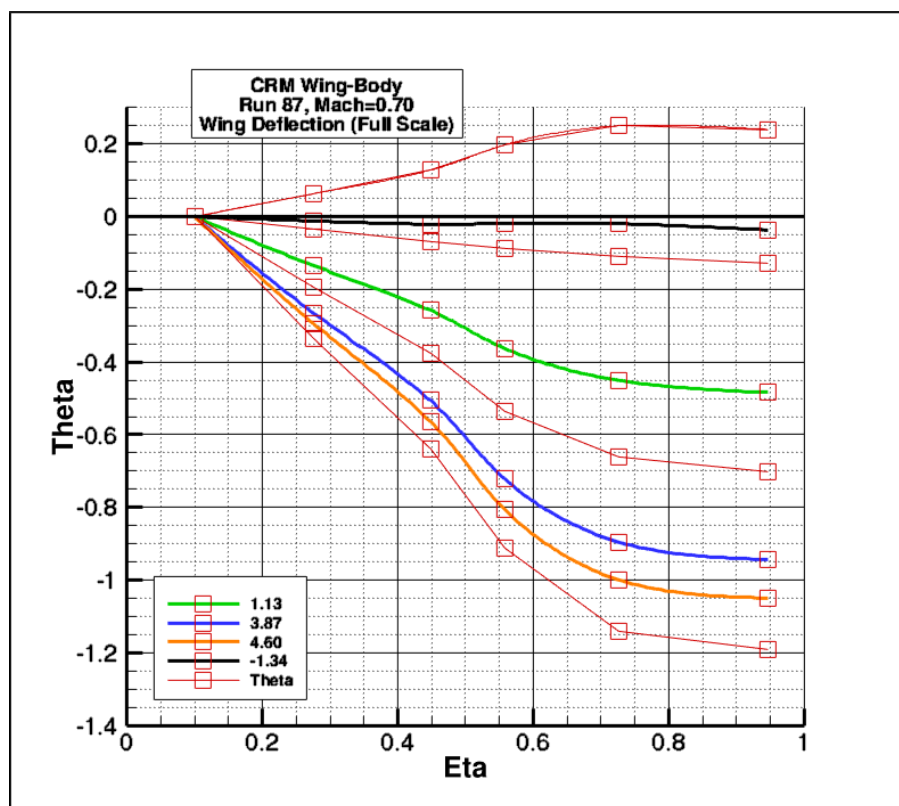


Figure 9 – Varying twist along the span of the wing for various angles of attack

In order to compare VSAERO's output to NASA's wind tunnel data, a CRM model consisting of a wing and body was used, as shown in Figure 10. This model was gridded using structured (quadrilateral) grids on the wings and part of the body and unstructured (triangular) grids on the remaining body, with a total of 3 structured patches and 11 unstructured patches. The model consists of 4983 body panels and 1754 wake panels.

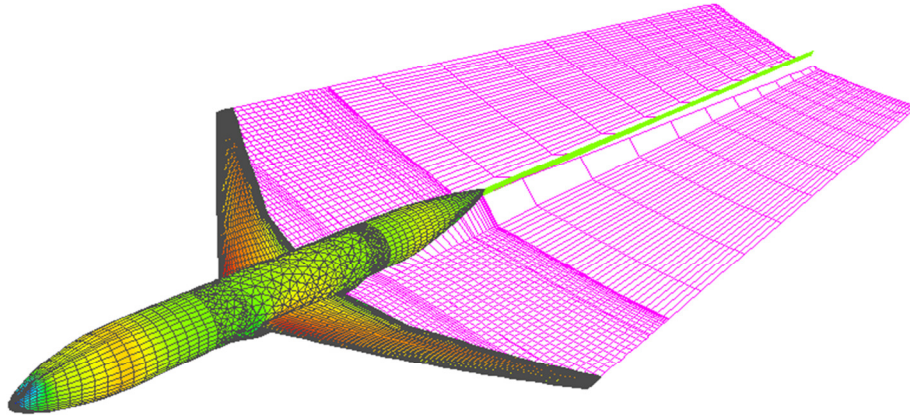


Figure 10 – CRM Wing-Body with grid and wake

Two sets of analyses of the CRM model were obtained through VSAERO. The first set consisted of analysis of the CRM at several angles of attack using the fixed geometry used for the Drag Prediction Workshop. The second set consisted of analysis of the CRM at several angles of attack using the measured wing twist distribution for each angle. The twist angles were taken from NASA's experimental data and applied to the geometry data using a 1st degree interpolation. Lift and pitching moment results for the two sets of analyses are shown in Figures 11 and 12. As indicated in reference 15, the wind tunnel data is subject to significant wind tunnel wall and mounting system interference and is not fully representative of "free-air". CFD results presented at the 5th Drag Prediction Workshop¹⁸ differed from the test data an average of approximately 0.5 degree in angle of attack for a given lift, and 0.05 in pitching moment coefficient. These increments were applied to the VSAERO results as uniform tares to angle of attack and pitching moment. The resulting VSAERO results show improved agreement with the test data with the inclusion of the aeroelastic twist in the CFD model

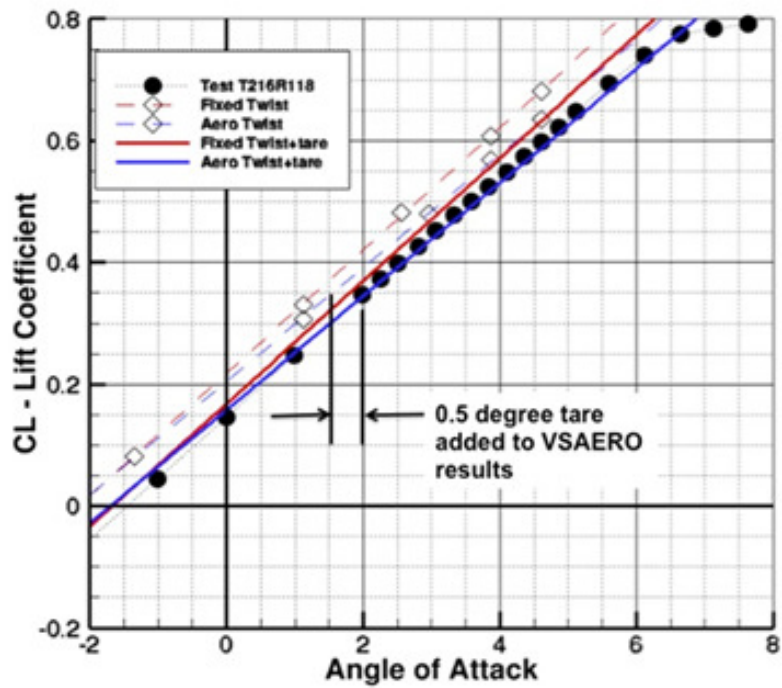


Figure 11 – CRM wing-body: angle of attack vs lift coefficient

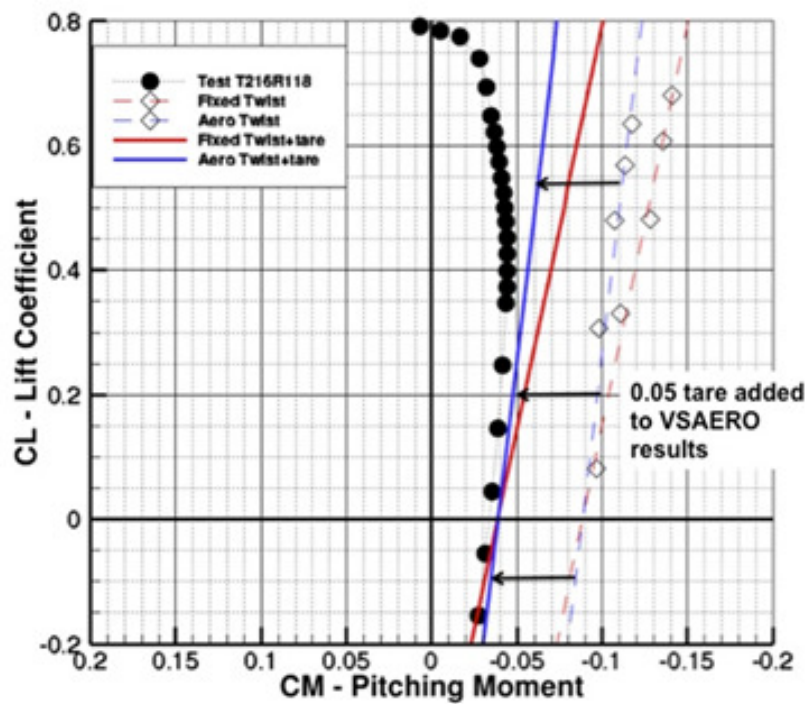


Figure 12 – CRM wing-body: pitching moment vs lift coefficient

The effects of including the aeroelastic twist in the solutions is most evident in the distribution of section lift coefficient along the span of the wing. This is illustrated in Figure 13 in which the wing section lift coefficient is plotted vs. the wing span fraction for both the fixed twist and the aero twist at the same angle of attack. The effect of the aeroelastic twist is to reduce the lift on the outboard portion of the wing. The experimental data has not been processed to yield the section force and moment characteristics, hence there is no experimental data to compare to.

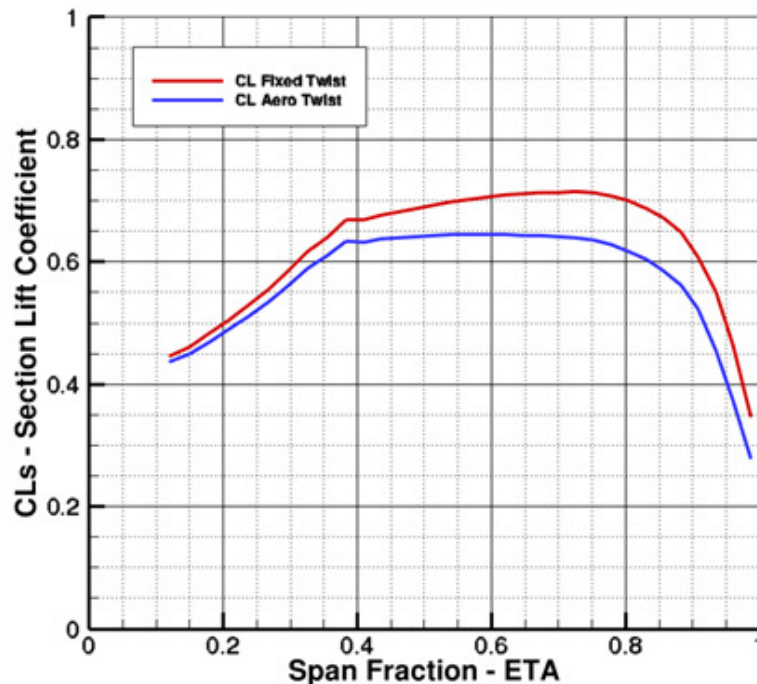


Figure 13 – CRM wing-body: section lift coefficient vs. wing span fraction.

4. CONCLUSIONS

Incorporating VSAERO's rapid analysis software into ANSA's user friendly pre and post processing environment will provide the users with an easily automatable and efficient preliminary design tool. The user will benefit from the time savings of ANSA's easy grid generation and VSAERO's rapid preliminary design analysis, coupled with the built in scripting functionality to automate processes.

REFERENCES

- (1) Nathman, J.K., "Subsonic Panel Methods – Second (Order) Thoughts", SAE 985563, Anaheim, CA 1998.
- (2) Maskew, B., "Prediction of Subsonic Aerodynamic Characteristics: A Case for Low-Order Panel Methods," *J. Aircraft*, Vol. 19, No. 2, February 1982.
- (3) Nathman, J.K., and Frank, J., "Application of VSAERO to Internal Flows," AIAA Paper 87-2415, Fifth Applied Aerodynamics Conference, Monterey, CA, 1987.
- (4) Hughes, M., "FSWAVE – A new module for VSAERO to model steady non-linear free surface flows", Analytical Methods, 1997.
- (5) Nathman, J.K., "Improvement of a Panel Method by including Panel Warp", AIAA 2004-0721, Reno, 2004.
- (6) Nathman, J.K., Induced Drag of High-Aspect Ratio Wings, AIAA 2005-1033, Reno.
- (7) Nathman, J.K., Hybrid Grid (Structured and Unstructured) Calculations with a Potential-based Panel Method, AIAA 2004-4836, Providence, 2004.
- (8) Nathman J. K., Potential-Based Panel Method for Oscillatory Motion, AIAA-2006-1255, 2006.
- (9) Morino, L., Kuo, C.C., "Subsonic Potential Aerodynamics for Complex Configurations. A General Theory", *AIAA Journal*, Vol. 12, 1974, pp. 191-97
- (10) Ehlers, F.E., Epton, M.A., Johnson, F.T., Magnus, A.E., and Rubbert, P.E., "A Higher Order Panel Method for Linearized Supersonic Flow," NASA CR-3062, 1979.
- (11) Riley, D.R., Wind-Tunnel Investigation and Analysis of the Effects of End Plates on the Aerodynamic Characteristics of an Unswept Wing, NACA TN 2440, 1951.
- (12) Vassberg, J. C., DeHaan, M. A., Rivers, S. M., and Wahls, R. A., "Development of a Common Research Model for Applied CFD Validation Studies," AIAA Paper 2008-6919, 26th AIAA Applied Aerodynamics Conference, Hawaii, HI, August 2008.
- (13) Vassberg, J. C., Tinoco, E. N., Mani, M., Rider, B., Zickuhr, T., Levy, D.W., Brodersen, O., Eisfeld, B., Crippa, S., Wahls, R. A., Morrison, J. H., Mavriplis, D.J., and Murayama, M., "Summary of the Fourth AIAA CFD Drag Prediction Workshop," AIAA Paper 2010-4547, June 2010.
- (14) Levy, D.W., Laflin, K. R., Vassberg, J. C., Tinoco, E. N., Mani, M., Rider, B., Rumsey, C., Wahls, R. A., Morrison, J. H., Brodersen, O., Crippa, S., Mavriplis, D.J., and Murayama, M., "Summary of the Fifth AIAA CFD Drag Prediction Workshop," AIAA Paper 2012-xxxx, June 2012.
- (15) Rivers, M., Hunter, C., and Campbell, R., "Further Investigation of the Support System Effects and Wing Twist on the NASA Common Research Model," AIAA Paper 2012-3209, June 2012.